

Hysteretic response of the electron-nuclear spin system in single $\text{In}_{0.75}\text{Al}_{0.25}\text{As}$ quantum dots: Dependences on excitation power and polarization

R. Kaji,¹ S. Adachi,^{1,2,*} H. Sasakura,² and S. Muto^{1,2}¹*Department of Applied Physics, Hokkaido University, N13 W8, Kitaku, Sapporo 060-8628, Japan*²*CREST, Japan Science and Technology Agency, Kawaguchi 332-0012, Japan*

(Received 10 September 2007; revised manuscript received 26 November 2007; published 24 March 2008)

Optically pumped nuclear spin polarization in single InAlAs quantum dots was investigated in detail with regards to the dependences on the excitation power and electron spin polarization. By increasing (or decreasing) the excitation power at a particular excitation polarization, an abrupt rise (or drop) and a clear hysteretic behavior were observed in the Overhauser shift of the photoluminescence under an external magnetic field of 5 T. Those features appear equivalently for the exciton and exciton complexes of the same quantum dot since the created nuclear field is equally effective. However, the degree of circular polarization shows different behaviors between a positively charged exciton and a neutral exciton or biexciton; further, only the positively charged exciton exhibits the precisely synchronized change and hysteretic behavior. It is suggested that the electron spin distribution is affected by the flip-flop of electron-nuclear spins. Further, the hysteresis is observed as a function of the degree of circular polarization of the excitation light, and its dependence on the excitation power is studied. The saturation of the Overhauser shift indicates the almost complete cancellation of the external magnetic field by the nuclear field.

DOI: [10.1103/PhysRevB.77.115345](https://doi.org/10.1103/PhysRevB.77.115345)

PACS number(s): 73.21.La, 78.67.Hc, 71.35.Pq, 71.70.Jp

I. INTRODUCTION

Recently, research on electron-nuclear spin interaction has been revived in view of its applications. This is because semiconductor quantum dots (QDs) enhance the electron-nuclear spin interaction (hyperfine interaction) due to their strong three-dimensional confinement of the electron wave function, and the enhanced interaction gives the possibility of aligning nuclear spins in one direction up to several tens of percent in a single QD through the optical pumping. In fact, a large rate of nuclear spin polarization and the resultant large effective nuclear field up to several tesla were observed recently in interface GaAs QDs,^{1,2} self-assembled InAlAs QDs,³⁻⁵ and InGaAs QDs.⁶⁻⁸ Because of the ultralong coherence, nuclear spin is expected to contribute to applications such as a long-lived quantum memory at the nuclear level⁹ and qubit conversion by using the nuclear field.¹⁰ Beyond such potential applications for quantum information processing, nuclear magnetic ordering and optically induced ferromagnetic ordering of spin systems are of surpassing interest in fundamental physics. Therefore, the control of nuclear spins in nanostructures has both fundamental as well as practical significance.

In this study, we investigated the optical pumping of nuclear spin polarizations in a single self-assembled InAlAs QD. An abrupt rise and the hysteresis of the Overhauser shift in addition to the degree of circular polarization (DCP) in the photoluminescence (PL) of positively charged excitons were clearly observed in the excitation power and excitation polarization dependences. Although the bistable behavior of the nuclear spin polarization on the excitation power was previously reported in single InGaAs QDs, the clear hysteretic response on the excitation polarization and the synchronized change of DCP are highlighted in the present work. Additionally, with the aid of this abrupt change, the sign of the electron g factor in the z direction is determined. Compared

with InGaAs QDs, the observed InAlAs QDs have the opposite sign and the smaller magnitude of the electron g factor despite the nearly same hole g factor. Since the saturated values of Overhauser shift (OHS) in InAlAs QDs and InGaAs QDs are almost the same ($\sim 100 \mu\text{eV}$), the larger external magnetic field can be compensated in InAlAs QDs. This situation, i.e., the electron states are degenerate and the hole states split largely, is preferable for the quantum bit conversion that is one of our research purposes.

II. SAMPLE AND EXPERIMENTAL SETUP

The QD sample was grown on a (100) GaAs substrate by molecular-beam epitaxy in the Stranski-Krastanow growth mode. The sample has an $\text{In}_{0.75}\text{Al}_{0.25}\text{As}$ QD layer embedded in $\text{Al}_{0.3}\text{Ga}_{0.7}\text{As}$ barrier layers.³ By atomic force microscopy measurements on a reference uncapped sample with the same growth condition, we found the average QD diameter of ~ 20 nm, height of ~ 4 nm, as well as areal QD density of $\sim 5 \times 10^{10}$ dots/cm².

For the single QD spectroscopy, small mesa structures with a typical top lateral size of ~ 150 nm were fabricated. A cw Ti:sapphire laser beam traveling along the QD growth direction was focused on the sample surface by a microscope objective. Time-integrated PL was measured at 5 K under the magnetic field of up to 5 T in the Faraday geometry. The PL from QDs was dispersed by a triple-grating spectrometer, and it was detected by a liquid-nitrogen-cooled Si charge coupled device camera with the typical exposure time of 1 s. The system resolution was found to be $12 \mu\text{eV}$, and the spectral resolution that determines the resonant peak energies was observed to be less than $5 \mu\text{eV}$ by using the spectral fitting.

III. RESULTS AND DISCUSSION

The PL spectra of a target single InAlAs QD at 0 T are shown in Fig. 1(a). The spectra were obtained for the wetting

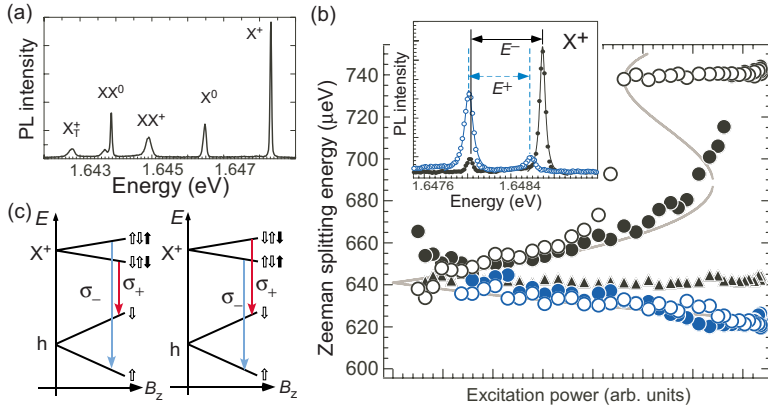


FIG. 1. (Color online) (a) PL spectra of a single QD at 0 T (5 K). (b) Excitation power dependence of E^+ , E^- (circles), and E^L (triangles) measured in the direction of increasing (solid marks) and decreasing (open marks) excitation powers at 5 T. The PL spectra at a given excitation power are indicated in the inset. (c) The Zeeman splitting in the Faraday geometry and PL transitions of X^+ for $g_z^e \cdot g_z^h > 0$ (left) and $g_z^e \cdot g_z^h < 0$ (right) assuming $|g_z^e| < |g_z^h|$. The solid (open) up arrows and down arrows represent electrons (holes) with the total angular momentum $J_{e,z}^c(J_{e,z}^v) = +\frac{1}{2}(+\frac{3}{2})$ and $J_{e,z}^c(J_{e,z}^v) = -\frac{1}{2}(-\frac{3}{2})$.

layer (WL) excitation (~ 730 nm) by using depolarized light. The figure shows almost all the emission lines from an isolated QD for the WL excitation with the moderate power. Through various measurements for the assignment of the PL spectra,¹¹ we conclude that the PL lines in the figure originate from the same single QD and can be attributed to X_T^+ (triplet state of a positively charged exciton), XX^0 (neutral biexciton), XX^+ (positively charged biexciton), X^0 (neutral exciton), and X^+ (singlet state of a positively charged exciton) from the low-energy side. The binding energies are $+2.5$ and -1.8 meV for XX^0 and X^+ , respectively. Furthermore, X^0 has a bright exciton splitting of 33 ± 5 μeV due to the anisotropic exchange interaction (AEI). Hereafter, we focus on the X^+ PL because the strongest PL is emitted in the case of WL excitation. X^+ consists of spin-paired holes and an electron whose spin is selectively created by circular excitation. Since X^+ has no dark states and since the spin-flipped electron can radiatively recombine with a hole immediately, the cycle rate for the electron-nuclear spin-flip-flop process under cw excitation is limited by the spin-flip rate of the single-hole state or the trion escape rate from the QD. On the other hand, in the case of X^0 , both bright and dark excitons can contribute to create the nuclear spin polarization, and the rate of spin flip-flop is limited by the long lifetime of the dark state in the case of the WL excitation. From the abovementioned features, the DCP of the X^+ PL is assumed for probing the electron spin directly. Therefore, the change of electron spins may become a mirror image of the change of nuclear spins. This argument will be tested later.

Figure 1(b) shows the excitation power dependence of E^+ , E^- , and E^L for X^+ at 5 T. We define E^+ , E^- , and E^L as the respective Zeeman splitting energies for σ_+ , σ_- , and linearly polarized excitations. The difference $E^{+(-)} - E^L$ is known as the OHS,¹² and it can be explained by considering the optical pumping of nuclear spin polarization and the resulting nuclear magnetic field. Since the total magnetic field experienced by X^+ is the sum of the external magnetic field B_z and nuclear field B_N , and since B_N acts only on electrons due to the nonzero existence probability at a nucleus site, the Zeeman splitting for circular excitation in Faraday geometry can be written as $E^{+(-)} = g_z^h \mu_B B_z + g_z^e \mu_B (B_z \pm B_N)$, where $g_z^{h(e)}$ is the hole (electron) g factor in the z direction and μ_B is the Bohr magneton. We can safely neglect the effect of B_N for the hole because the hole does not have the existence prob-

ability at the nucleus site due to its p -like wave function.¹⁰ The equation says that the OHSs, $E^{+(-)} - E^L$ should have opposite sign, but be the same quantity corresponding to $\pm B_N$ if $\pm B_N$ does not depend on the excitation light polarization. In fact, such a symmetric OHS ($|E^+ - E^L| = |E^- - E^L|$) has been observed in previous studies.^{1,3-5} However, in this single InAlAs QD, $E^+ - E^L \sim -20$ μeV and $E^- - E^L \sim +100$ μeV . This means that B_N is different for σ_+ and σ_- excitations. The solid (open) marks indicate the Zeeman energies measured in the direction of increasing (decreasing) excitation power. While E^+ (E^L) indicates the gradual change (no change) with an increasing or decreasing excitation power, E^- shows the abrupt change and bistable behavior on the excitation power. Such bistable behavior is observed only for E^- in the B_z range of 2–5 T. Besides, the OHS of 100 μeV corresponds to the nuclear spin polarization rate of $\sim 30\%$ assuming the equal contribution of all nuclear species and the maximum value of 295 μeV OHS for $\text{In}_{0.75}\text{Al}_{0.25}\text{As}$ QDs.

Recently, the similar bistable behavior of the OHS was observed for X^0 in InGaAs/GaAs QDs for an excitation power in the range of 1–3 T.⁷ While, in a recent study, an abrupt change was observed in a decreasing E^+ , in the data presented here, an abrupt change appears only in E^- . This difference is due to the sign of g_z^e in the InAlAs QD ($g_z^e \sim -0.37$),¹³ which is opposite to g_z^e in an InGaAs QD ($g_z^e \sim +0.60$). As observed in Fig. 1(c), the Zeeman splitting of X^+ PL is given as $E_Z^h + E_Z^e$ for $g_z^e > 0$ and $E_Z^h - E_Z^e$ for $g_z^e < 0$, where $E_Z^{h(e)}$ is the Zeeman splitting energy of a hole (an electron). Therefore, increasing the Zeeman splitting of E^- in Fig. 1(b) signifies a *reduction* in the electronic Zeeman energy E_Z^e of X^+ due to the compensation of B_z by B_N . Hence, our observation and the recent findings are interpreted as follows. An abrupt change occurs only when B_N reduces the external field B_z , and therefore the same physics is considered to underlie the observed bistable behavior.

The optical pumping of the nuclear spin polarization is described by the following rate equation:^{14,15}

$$\frac{d\langle I_z \rangle}{dt} = \frac{1}{T_{\text{NF}}} [Q(\langle S_z \rangle - S_0) - \langle I_z \rangle] - \frac{1}{T_{\text{ND}}} \langle I_z \rangle, \quad (1)$$

where $\langle I_z \rangle$ and $\langle S_z \rangle$ are the averaged nuclear and electron spin polarizations, S_0 the thermal electron spin polarization, $1/T_{\text{NF}}$ and $1/T_{\text{ND}}$ nuclear spin polarization and depolariza-

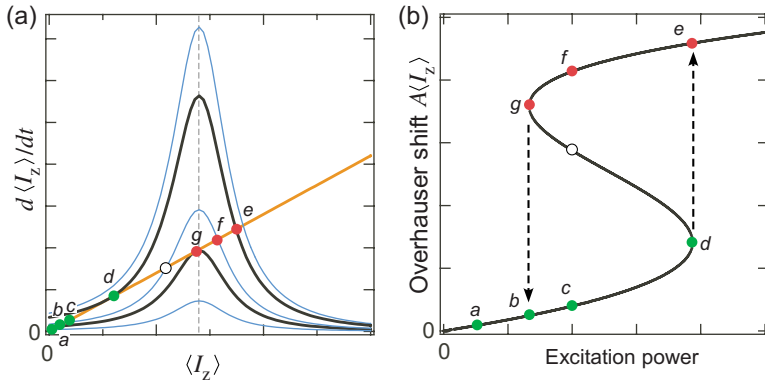


FIG. 2. (Color online) (a) Graphical representation of excitation power dependence of OHS. The steady-state nuclear polarization is determined by the balance between the polarization (Lorentzian shape) and the depolarization (straight line) terms. The thick curves represent the polarization terms at the low and high threshold excitation powers. (b) Bistable behavior of the steady state $\langle I_z \rangle$. The states $a-g$ correspond to those in (a).

tion rates, and $Q(=[I(I+1)]/[S(S+1)])$ is the momentum conversion coefficient from an electron spin to a nuclear spin system. Nuclear spin diffusion is included in the depolarization term. Based on the general form of the spin-flip process in the precessional decoherence type,¹⁴ the spin transfer rate $1/T_{NF}$ is given as follows by assuming the uniform electron wave function in a QD:^{6,7}

$$\frac{1}{T_{NF}} = \left[f_e \tau_c \left(\frac{A}{N\hbar} \right)^2 \right] / \left[1 + \left(\frac{\tau_c}{\hbar} \right)^2 (g_z^e \mu_B B_z \pm A \langle I_z \rangle)^2 \right], \quad (2)$$

where A , N , and f_e are the hyperfine coupling constant, number of nuclei, and filling factor of X^+ in the QD, respectively. Here, the filling factor f_e is determined as $f_e = n_e \tau_c / \tau_R$, where n_e and τ_R is the electron density of X^+ in the QD and lifetime of X^+ . τ_c is the correlation time of the coupled electron-nuclei system with a broadening \hbar/τ_c that is basically decided by the shortest time of the electron-hole recombination, spin relaxation, and spin tunneling out of the QD. Here, $g_z^e \mu_B B_z \pm A \langle I_z \rangle [= g_z^e \mu_B (B_z \pm B_N)]$ represents E_Z^e affected by B_N . According to the Eq. (2), the external field compensation by a nuclear field decreases E_Z^e and accelerates the spin transfer from electrons to the nuclei at a particular polarization. In this simple model, the coupled electron-nuclear spin system shows a static hysteresis loop in the relation between the OHS ($=A \langle I_z \rangle$) and three variable parameters: n_e (\propto excitation power), $\langle S_z \rangle$ (\propto excitation polarization), and B_z . It is worth pointing out that Eq. (2) can be revised somewhat by considering the electron-hole exchange interaction. In the case where the electron-nuclear flip-flop transition takes place in the presence of the unpaired hole spin, e.g., neutral exciton, electron spin experiences additional effective magnetic field (B_J) created by the hole spin via exchange interaction. Considering the typical value of the energy splitting between the bright and dark states of $\sim 100 \mu\text{eV}$, this energy splitting is comparable to the width of the formation term; hence, the nuclear spin-flip rate will be affected by B_J .¹⁶ The electron-hole exchange interaction is thought to play significant role in the dynamics of nuclear spin polarization,¹ and it is important to evaluate B_J in more detail. Though we think that B_J depends not only on the bright-dark energy splitting but also to hole relaxation time at present, this topic is our next step and then we will add the detailed rate equation of the electronic system.

In the next figure, we consider the excitation power dependence of the OHS. The steady state $\langle I_z \rangle$ of Eq. (1) with the rate given by Eq. (2) along with a constant $1/T_{ND}$ is expressed graphically by the intersecting points of both the polarization and depolarization terms. The Lorentzian-shaped polarization term increases up with n_e . Starting from the point a , the intersection is unique and then, with *increasing* the excitation power, the steady state $\langle I_z \rangle$ follows the straight line of the depolarization term. Beyond point b , two new solutions appear; however, the system still remains in the low $\langle I_z \rangle$ state. At point d , this lower state disappears and the OHS jumps up to a new state e . For further increasing the excitation power, the state remains on the upper branch. The trajectory of the steady state $\langle I_z \rangle$ is depicted as a function of n_e in Fig. 2(b). In the case of a decreasing excitation power, the state on the upper branch remains down at the lower threshold power where the upper state g disappears and the system has to return to the lower state (point b). In the region between the low and high threshold powers, there are two stable $\langle I_z \rangle$; the realization of one of them depends on history, i.e., on whether one comes from higher or lower excitation power. The intermediate branch is unstable (e.g., open circle in the figure), and if the system is prepared by some means on this branch, the slightest deviation from the unstable branch due to a fluctuation causes the system to move into a state on the upper or lower stable branch. According to this model, the experimental data in Fig. 1(b) can be fitted with the solid gray curve by using the following parameters: $N = 4 \times 10^4$, $\tau_c = 18$ ps, $T_{ND} = 10$ ms, $\tau_R = 1$ ns, $g_z^e = -0.37$, $\bar{A} = 52.6 \mu\text{eV}$, and $\bar{I(I+1)} = 12.25$. Here, \bar{A} and $\bar{I(I+1)}$ are weighted averages for $\text{In}_{0.75}\text{Al}_{0.25}\text{As}$ QD. We take these values tentatively, even though the fluctuation of the contents within a QD is thought to be large and the accurate hyperfine coupling constant of Al has not been known at present. N is estimated from the averaged dot diameter and height assuming the lens-shaped QD. The τ_R and g_z^e are obtained for this QD by other experiments,¹³ and τ_c and T_{ND} are used as the fitting parameters. The fitting results of τ_c have a reasonable order of magnitude compared with the value (~ 45 ps) from the single photon Fourier spectroscopy.¹⁷

Figure 3 highlights the importance of X^+ . E^- for X^+ PL (left panel) and X^0 PL (right panel) shows the same bistable behavior and an abrupt change at exactly the same low and high threshold powers. It is not surprising since the created B_N is effective for the entire target single QD. Therefore, all

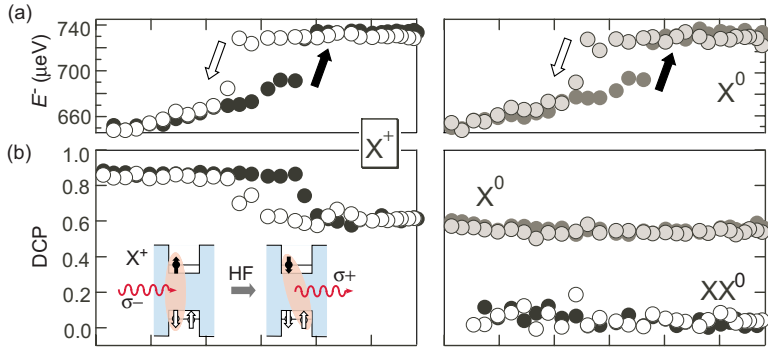


FIG. 3. (Color online) (a) Observed E^- as a function of the excitation power (5 K, 5 T). The black (white) arrows indicate the measurement direction of the power dependence plotted by the solid (open) circles. Hysteresis in E^- was observed for X^+ , X^0 , and XX^0 PL (E^- of XX^0 is not shown here, but it is almost the same as that of X^+ and X^0). (b) Observed hysteresis loop in the DCP for X^+ PL. This hysteresis can be observed for X^+ PL only (left), and it is not observed for X^0 and XX^0 PLs (right). Schematic of the σ_- excitation of X^+ and the emission after the spin-flip-flop process between an electron and a nucleus (inset).

excitations such as X^+ and X^0 with single electron in the same QD should feel the same B_N if they have the same g_z^e . However, the DCP of the PL is quite different for X^+ and X^0 , as observed in Fig. 3(b). Here, the DCP is defined as $(I^- - I^+) / (I^- + I^+)$, where I^{\pm} denotes the integrated PL intensity of the σ_{\pm} -polarized spectrum. Note that XX^0 PL has zero DCP although it is always a mirror image of X^0 PL in the Zeeman splitting energy. This is because XX^0 is not affected by B_z and B_N due to the spin-paired electrons and holes, and it has equal transition probabilities to the X^0 states with $J_z = \pm 1$.

While the DCP of X^+ shows the abrupt changes and hysteresis synchronized to those for the OHS, the DCP of X^0 shows no signature. These data clearly indicate that X^+ PL directly probes the electron spin. Generally, the external longitudinal magnetic field can significantly suppress the electron spin relaxation in the “internal random magnetic field” (IRMF) that originates from the effective magnetic fields resulting from the hyperfine interaction, exchange interaction, and spin splitting of the conduction band.¹⁴ Therefore, when $B_z - B_N = 0$, the above competing electron spin relaxation can emerge and reduce the steady state DCP. In fact, the DCP is ~ 0.35 and ~ 0 for X^+ and X^0 for 0 T in this QD. The difference between the DCPs for X^0 and X^+ is interpreted as follows. The DCP of X^0 is originally low because of the AEI. At 5 T, the DCP is improved to ~ 0.6 , and with an increase in B_N , it shows little change since the hole with a large

$g_z^h (\gg |g_z^e|)$ still feels B_z . On the other hand, the DCP of X^+ is intrinsically high due to the absence of the AEI between electron and spin-paired holes. The DCP is improved to ~ 0.95 at 5 T due to the suppression of the electron spin relaxation by the IRMF; however, it deteriorates after switching by the cancellation of B_z and the resulting revival of the suppressed relaxation. The origin of the IRMF in our QD has not been identified yet. However, the spin splitting of the conduction band is not likely because it is not expected to cause spin relaxation in QDs. Therefore, the hyperfine interaction is the most likely origin of the IRMF. The electron spin relaxation due to the hyperfine interaction is nothing but the term described by Eq. (2). Consequently, it indicates that the electron spin polarization is affected by the flip-flop of electron and nuclear spins.

Finally, the excitation polarization dependence of the Zeeman splitting and the DCP of X^+ at different excitation powers are shown in Fig. 4. We note that the excitation polarization controls one of the most important parameters of the rate equation of Eq. (1), i.e., $\langle S_z \rangle$. It indirectly controls the quantity $[Q(\langle S_z \rangle - S_0) - \langle I_z \rangle]$ in Eq. (1), the zero of which determines the equilibrium value of $\langle I_z \rangle$ in the limit of negligible $1/T_{\text{ND}}$. The value $\langle I_z \rangle = Q(\langle S_z \rangle - S_0)$, in the limit of the lowest order of hyperfine constant, is the one given by the detailed balance argument in the textbook.¹⁵ Therefore, the control of the light polarization presents an independent way of controlling the nuclear polarization switching in addition to the

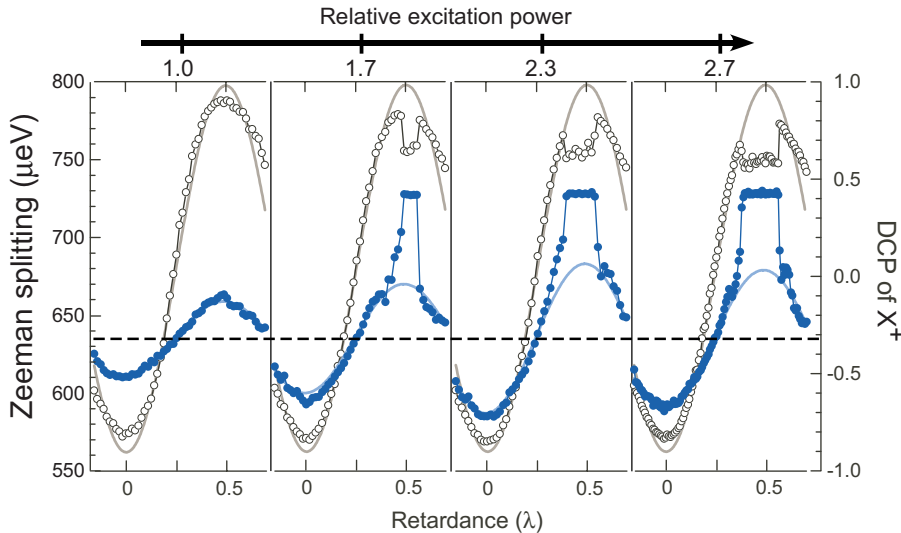


FIG. 4. (Color online) Variation in the Zeeman splitting energy that is affected by the nuclear field depending on the excitation polarizations (5 T, 5 K). The dashed line indicates the splitting E^L . The corresponding reduction in the DCP (open circles) is also observed. The retardances $\lambda=0$ and 0.5 correspond to the σ_+ and σ_- excitations, respectively.

excitation power and the external magnetic field both of which control the quantity $1/T_{\text{NF}}$. Unfortunately, in the present case, the control just resembles the excitation power dependence through the factor $n_e \langle S_z \rangle$ because $1/T_{\text{ND}}$ is not small and Q is large for an InAlAs QD. As a result, $\langle I_z \rangle$ can be neglected in the term $Q(\langle S_z \rangle - S_0) - \langle I_z \rangle$ and not in $\langle I_z \rangle / T_{\text{ND}}$.

In the leftmost panel, the Zeeman splitting and DCP follow the excitation polarization as $\cos(2\pi\lambda - \pi)$ centering on E^L ($\sim 640 \mu\text{eV}$) and S_0 (~ 0.05), respectively, where λ is the retardance that is generated by rotating a quarter-wave plate in the excitation laser path. This is a case under the threshold excitation power.³ As exceeding the threshold excitation power, the deviation from E^L (i.e., OHS) increases and the energy shift changes abruptly by up to $\sim 100 \mu\text{eV}$ around the σ_- excitation ($\lambda \sim 0.5$). In addition, the synchronized reduction of the DCP occurs. With a further increase in the excitation power, the region of saturation of the OHS and DCP increases according to the product $n_e \langle S_z \rangle$ and becomes asymmetrical about $\lambda = 0.5$, reflecting a bistable nature. It is worth pointing out that the maximum value of the OHS saturates as long as $n_e \langle S_z \rangle$ is above a given threshold. In the saturation region of OHS, as seen in Fig. 2(a), B_{N} balances with B_z within the half width \hbar/τ_c of the Lorentzian-shaped polarization rate. Therefore, this means that the width of the Lorentzian-shaped polarization rate is sufficiently small.

Within the range of B_z that the nuclear spin bistability is observed, the cancellation is achieved more perfectly as B_z increases, since the saturation occurs close to the top of Lorentzian-shaped polarization rate. This B_z cancellation by B_{N} for the electron leads to “zero effective g factor” that is essential for the quantum bit conversion.

IV. SUMMARY

In summary, we investigated the optical pumping of nuclear spin polarizations in a single InAlAs QD and observed the clear bistable behavior of the OHS of up to $\sim 100 \mu\text{eV}$ in the excitation power and polarization dependences at 5 T. The bistability can be seen only in the case of σ_- excitation and the behavior is explained by the simple model in which the rate of spin flip-flop between an electron and a nucleus depends on the electronic Zeeman splitting that is affected by the nuclear field. We found that X^+ PL directly probes the electron spin and therefore the DCP synchronizes the change in the OHS. It is suggested that the electron spin distribution is affected by the flip-flop of electron-nuclear spins. The saturated OHS shows the complete cancellation where the difference between the external magnetic field and the created nuclear field is within the narrow width of the Lorentzian function.

*adachi-s@eng.hokudai.ac.jp

- ¹D. Gammon, Al. L. Efros, T. A. Kennedy, M. Rosen, D. S. Katzer, D. Park, S. W. Brown, V. L. Korenev, and I. A. Merkulov, *Phys. Rev. Lett.* **86**, 5176 (2001).
- ²A. S. Bracker, E. A. Stinaff, D. Gammon, M. E. Ware, J. G. Tischler, A. Shabaev, A. L. Efros, D. Park, D. Gershoni, V. L. Korenev, and I. A. Merkulov, *Phys. Rev. Lett.* **94**, 047402 (2005).
- ³T. Yokoi, S. Adachi, H. Sasakura, S. Muto, H. Z. Song, T. Usuki, and S. Hirose, *Phys. Rev. B* **71**, 041307(R) (2005).
- ⁴T. Yokoi, S. Adachi, H. Sasakura, S. Muto, H. Z. Song, T. Usuki, and S. Hirose, *Physica E (Amsterdam)* **29**, 510 (2005).
- ⁵T. Mukumoto, R. Kaji, H. Sasakura, S. Adachi, H. Kumano, S. Muto, and I. Suemune, *Phys. Status Solidi C* **3**, 4372 (2006).
- ⁶P.-F. Braun, B. Urbaszek, T. Amand, X. Marie, O. Krebs, B. Eble, A. Lemaitre, and P. Voisin, *Phys. Rev. B* **74**, 245306 (2006).
- ⁷A. I. Tartakovskii, T. Wright, A. Russell, V. I. Falko, A. B. Van'kov, J. Skiba-Szymanska, I. Drouzas, R. S. Kolodka, M. S. Skolnick, P. W. Fry, A. Tahraoui, H.-Y. Liu, and M. Hopkinson, *Phys. Rev. Lett.* **98**, 026806 (2007).
- ⁸P. Maletinsky, C. W. Lai, A. Badolato, and A. Imamoglu, *Phys. Rev. B* **75**, 035409 (2007).
- ⁹J. M. Taylor, C. M. Marcus, and M. D. Lukin, *Phys. Rev. Lett.*

90, 206803 (2003).

- ¹⁰S. Muto, S. Adachi, T. Yokoi, H. Sasakura, and I. Suemune, *Appl. Phys. Lett.* **87**, 112506 (2005).
- ¹¹H. Kumano, S. Kimura, M. Endo, H. Sasakura, S. Adachi, S. Muto, and I. Suemune, *J. Nanoelectron. Optoelectron.* **1**, 39 (2006).
- ¹²A. W. Overhauser, *Phys. Rev.* **92**, 411 (1953).
- ¹³It is worth pointing out that the abrupt change in the OHS can be used to obtain the magnitude and the sign of g_z^e . We obtained $g_z^e = -0.37 \pm 0.02$ and $g_z^h = 2.54 \pm 0.01$ for this InAlAs QD by measuring the abrupt change in the OHS; for this B_z was scanned at several values of the excitation power. See R. Kaji, S. Adachi, H. Sasakura, and S. Muto, *Appl. Phys. Lett.* **91**, 261904 (2007).
- ¹⁴*Optical Orientation*, edited by F. Meier and B. Zakharchenya, *Modern Problems in Condensed Matter Sciences Vol. 8* (North-Holland, New York, 1984), Chaps. 2 and 5.
- ¹⁵A. Abragam, *The Principles of Nuclear Magnetism* (Clarendon, Oxford, 1961).
- ¹⁶I. A. Merkulov, *Phys. Usp.* **45**, 1293 (2002).
- ¹⁷S. Adachi, H. Sasakura, N. Yatsu, R. Kaji, and S. Muto, *Appl. Phys. Lett.* **91**, 161910 (2007).